MODAL TEST OF THE CASSINI SPACECRAFT

Kenneth S. Smith* and Chia-Yen Peng†

*SDRC Operations, Inc.
11995 El Camino Real, Suite 200
San Diego, CA 92130

†Jet Propulsion Laboratory
California Institute of Technology
4800 Oak Grove Drive
Pasadena, CA 91109

ABSTRACT, *Modal testing of the Cassini spacecraft posed a challenge due to the large size and dynamic complexity of the spacecraft. A successful test required careful pre-test analysis, the use of a variety of testing methods, and flexibility in responding to unexpected behavior. The test brought some surprises, including nonlinear behavior of a critical mode which required a follow-tip high level test. This paper presents an overview of the test methods and rc.suits, with an emphasis on* lessons *learned*

NOMENCLATURE

DOF	Degree(s) of Freedom
FEM	Finite Element Model
FPP	Fields and Particles Pallet
FRF	Frequency Response Function
HGA	High Gain Antenna
JPL	Jet Propulsion Laboratory
LEM	Lower Equipment Module
LSA	Linear Separation Assembly
LVA	Launch Vehicle Adapter'
PMS	Propulsion Module Subsystem
RSP	Remote Sensing Platform
TAM	Test Analytical Model
Uss	Upper Shell Structure

J. INTRODUCTION

A modal test was performed on the Cassini spacecraft at the Jet Propulsion Laboratory in August 1995[1,2]. The objective of the task was to provide experimental data for the verification of the firrite element model (FEM) of the space.cmt't in its launch configuration. A test.verified model must he approved prior to the final coupled loads analysis and subsequent launch approval.

The specific test objective was to measure the frequency, damping, and mode shape of all significant modes of the Cassini spacecraft test article below 70 Hz, with the structure fixed at its interface to the Centaur upper stage, Significant modes were defined as modes whose e. ffective mass was at least 5% of [he total rigid mass of the spacecraft.

'Ibis paper gives art overview of the modal test methods and results, with art emphasis on the lessons learned during the test.

2. TEST ARTICLE

The Cassini spacecraft is by far the largest interplanetary spacecraft ever developed, with a total launch mass of 5600 kg (propellants account for more than 3100 kg of this total). The spacecraft will be launched on October 6, 1997, on a Titan IV/Centaur launch vehicle, and will reach Saturn in the year 2,004. At that time, the main engine will place the spacecraft into Saturn orbit, and a four year tour of the Saturnian system will begin, Foremost among the mission objectives is the delivery of the 315 kg Huygens probe into the dense atmosphere of Titan, which is the largest of Saturn's moons and is nearly the size of the planet Mars,

Early project plans had called for the modal test to be performed on the flight article, after integration of the flight electronics and science instruments. This plan was intended to minimize the cost of additional hardware for test, but would have made the modal test much more difficult, due to the handling constraints on flight electronics. It would also have greatly compressed tile schedule for model correlation. Fortunately, the program was replanned to allow a develop. ment test program prior to integration of the flight article.

The Cassini spacecraft structure (Figure 1) is assembled from several components: the conical launch vehicle adapter; the linear separation assembly; the lower equipment module, which supports reaction wheels and radioisotope thermoelectric generators; the propulsion module subsystem. including the large fuel and oxidizer tanks (inside the cylindrical core): the upper shell structure, which supports the two instrument platforms and other equipment: and the bus, which houses and protects the electronic heart of the spacecraft. The high gain antenna is mounted above the bus, and the Huygens probe is supported by a truss attached to the propulsion module.

The test article assembled for the modal test (Figure 2) was a combination of flight hardware (LVA, L. FM, USS, FPP, RSP, bus, and most trusses), flight-like hardware (l-SA), development test hardware (PMS, HGA, probe), and mass

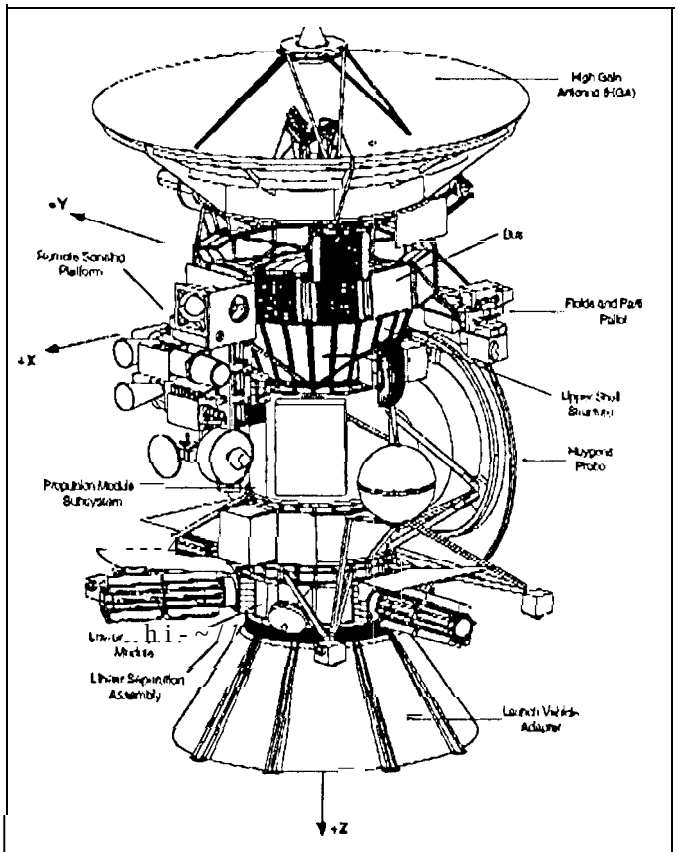

Figure 1. Cassini spacecraft structural components.

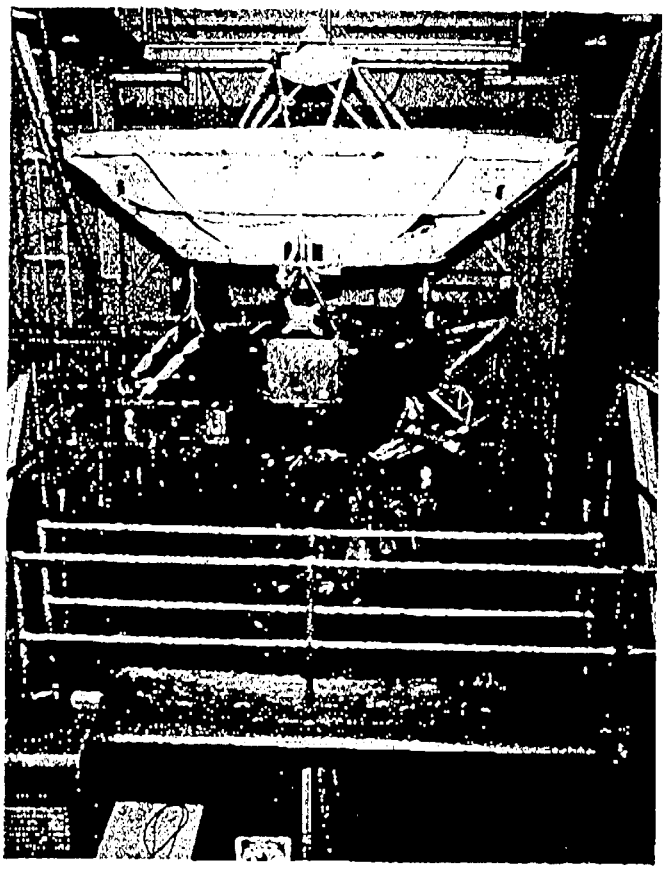

Figure 2. Cassini test article in modal pit.

mockups (instruments, reaction wheels, electronics boxes, cabling, etc.). No liquid propellants were present, since the various tanks were not yet available. The 3000 kg mass of the oxidizer and fuel tanks wrrs represented by steel ballast. (Propellant slosh modes will be added to the flight model based on analysis and slosh testing.)

Fixed boundary conditions were enforced by bolting the spacecraft to the seismic mass in the modal pit of JPL's Environmental Test Facility. At a height of over 16.7 m (22 ft), the test article was a tight fit.

3. PRE-TEST ANALYSIS

Critical [o the test effort was the development of a Test Analytical Model. or TAM, for the test configuration, The starting point for the TAM was the NASTRAN model of the flight configuration, which had been maintained throughout [he spacecraft development process, The main task in developing the TAM was tracking and incorporating the ninny changes between the test article and the flight article. Painstaking attention was paid to the mass mockups, including direct measurement of the mass of each mockup. and solid modeling to determine the c.g. and moments of inertia. This attention to detail proved to be important for later orthogonality calculations using the analytical mass matrix.

The TAM incorporated air mass effects on the HGA, which tends [o lower the frequencies of the antenna modes. No . corrections as discussed in [3] were required for the TAM, ' because the base of the spacecraft was fixed,

The pre-test TAM served a number of purposes:

1. It was used to predict test modes for test planning. including shaker location selection;
2. It was used to help assess the adequacy of the planned instrumentation;
3. The TAM was also used during the test to expand mode shape measurements to full model size for visualization;
4. The Guyan-reduced mass matri x from the TAM was used for orthogonality and effective mass calculations for the test mode shapes;
5. It formed the basis for the model correlation

The pre-test analysis predicted 7S modes of the test article below 70 Hz, starting at 7,7 Hz, The test modes were sorted by effective mnss to help in identifying significant modes that should be targeted during the test.

4. 1NSTRUMENTATION

The data acquisition and test control system used for the test was a Zonic Workstation 7000 with an HP/735 workstation acting as host computer, The Zonic front end provided four independent output channels, and 80 input channels. Post processing of the test data, including curve-fitting and mode shape animation, was done on the HP workstation using SDRC I-DEAS software,

A total of 256 accelerometers (PCB Structcels and Flexcels) were installed for the test at 135 different locations, This number was chosen based on the capacity of the bank-switching system, which can switch *4* banks of 64 channels each. Each acquisition pass captured one of these banks, along with four input force measurements, four drive point accelerometers, and eight other repeating measurements used for protection of the test article,

Accelerometer locations were selected by a combination of mathematical optimization methods and engineering judgment. The primary numerical criterion for evaluating candidate locations was the orthogonality product $\Phi^T M \Phi$, where Φ is the matrix of mode shapes from the TAM. partitioned to the measurement DOF, and M is the reduced mass matrix obtained by Guyan reduction of the TAM mass matrix to the measurement DOF. Ideally this product should produce an identity matrix. The measurement set was evaluated based on maximizing the diagonal terms and minimize the off-diagonal terms of this matrix.

One annoyance in the pre-test analysis was that many of the large mass items (instruments, electronic boxes) were modeled as lumped masses which were attached to their structural supports through rigid elements. As a result, many of the natural candidate accelerometer locations were dependent DOF in the model. In order to perform Guyan reduction, the rigid elements would have had [o be rewritten to make the lumped mass the independent DOF. There were so many candidate locations with this problem that a special NASTRAN DMAP sequence was developed which allowed Guyan reduction to be performed when the measurement set included dependent DOF, The technique required that both sides of a rigid clement could not be instrumented,

Because the total number of accelerometers was limited, a large number of locations had only one or two axes measured. Also, rotated coordinate systems were used extensively. For example, on the HGA main reflector, most of the accelerometers measured motion normal to the dish, which involved different coordinate axes at each point. Although this scheme maximized the usefulness of the 256 accelerometer measurements, the large number of coordinate systems was a significant source for errors that later had to be tracked down.

Correspondence between test DOF and FEM DOF was maintained by introducing all test coordinate systems into the TAM. Grid points were added to the model at each instrumented point, and the displacement coordinate systems of the added nodes were set to match the accelerometer orientations in the test. Because of the ability to perform Guyan reduction with dependent DOF, all of the test DOF were made dependent on FEM DOF, usually at coincident nodes. 'This scheme avoided the problems that would have been created had we changed displacement coordinate systems of the original FEM nodes.

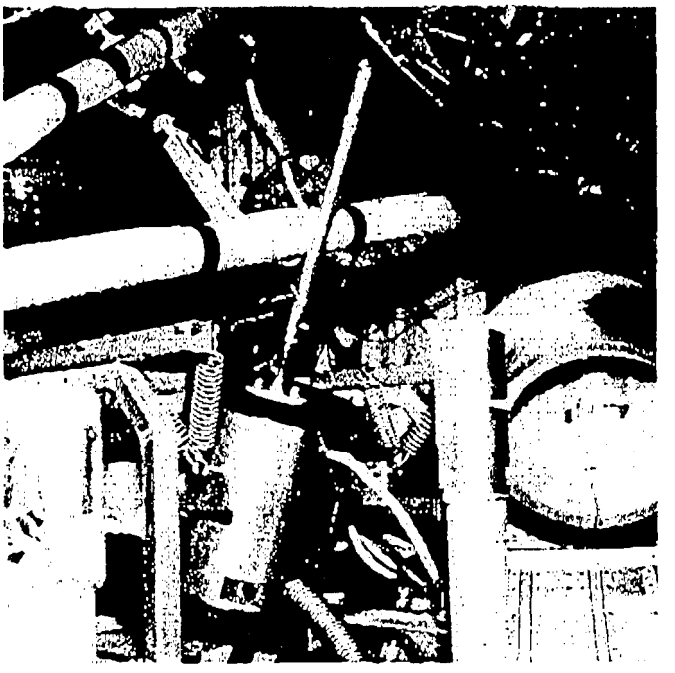

Figure 3, Shaker (in isolation cage) attached to probe.

Accelerometer calibration and installation on the structure was automated by the use of a bar coding scheme. Each transducer was bar coded, as well as every instrumented location. Cable routing was determined automatically as transducers were installed, by interrogation of the signal conditioners by the workstation. This system virtually eliminated most common test setup errors, but human error was still possible in identification of transducer orientation and coordinate system definitions, The task of relating test coordinate systems back to the NASTRAN model was a significant or-m, and consumed a great deal of the allocated testing time.

Excitation was provided by four VTS100 lbf electrodynamic shakers. The shakers were suspended on soft springs in cages, providing isolation from the ground support (see Figure 3). Attachment to the structure was made at various structural hard points on the bus, RSP, and Huygens probe. Shaker locations and orientations were selected based *on* pre-test analysis and preliminary test measurements. Nine different locations/orientations were used in the test.

5. TEST METHODS

The overall test strategy involved a combination of the burst random and stepped sine techniques, A number of broadband surveys (up to 70 Hz) were performed using burst ran. dom excitation from four shakers. Different shaker locations and force levels were applied. Each test was repeated four times in order to acquire all 256 response channels. Frequency response functions (FRF's) were stored by the Zonic software in binary files suitable for input to the I-DEAS pro. gram.

Modal parameters (frequency, damping, mode shape) were estimated from the broadband FRF's using the polyreference Lime domain method. Visualization of the mode shapes required expansion of the measured DOF to the full model size. The expansion was performed using the inverse of Guyan reduction — equivalent to enforcing the modal deflection at measured DOF and computing the motion of all other DOF based on static stiffness.

Examination of mode shape plots revealed some error-s in coordinate systems that were corrected in the TAM, The. process of' identifying errors and debugging coordinate systcm definitions was slow and tedious, and could not be completed until preliminary burst random data was acquired. This meant that this debugging process consumed part of the scheduled time for testing.

After correcting setup errors and obtaining good broadband data sets, linearity testing of the 15 most significant modes was performed. The objective of this part of the test was to explore. differences between the modal parameters at low level (as measured in the broadband burst random testing) and at higher response levels.

An ideal technique for this type of testing is stepped sine, where one or more shakers excite the structure at a single frequency, and the. FRF's at that frequency are measured before stepping to the next frequency, This excitation method provided the ability to generate relatively large response amplitudes within the limited capability of the shaker system. Unfortunately, due to communications problems the Zonic sine testing implementation was extremely slow. In order to keep test times within reasonable limits, sine testing, could be performed with a single shaker only, and only one of the four banks of data was usually acquired, These limitations made this technique undesirable when there were multiple closely spaced modes. Stepped sine testing was performed On severe significant modes — primary cure bending, torsion, two major axial modes, Huygens probe bounce, and RSP bounce. In each case, excitation force was varied over at least an order of magnitude to see its effect on natural frequencies and damping.

A different approach was used for the remaining significant modes. where multiple closely spaced modes would have made it difficult to extract reliable frequencies from single-shaker data. For the other modes, high level narrow-band burst random excitation was applied using three or four shakers, Reduction of bandwidth allowed a greater amount of energy to be applied to the targeted modes, For each shaker, the RMS force level over the narrow frequency band was one to two orders of magnitude higher than for the broadband in the same frequency range. In these tests, full response data was taken in four banks, allowing comparisons of mode shapes as well as frequency.

6. PROBE NONLINEARITY

The stepped sine testing revealed an unusually severe nom linearity in the bounce mode of the probe. near 19 Hz (Figure 6). The apparent problem was that the frequency was dropping with increased force level, and did not show signs of leveling off within our excitation capability, The highest level test produced a response in the probe approximately 10% of expected flight acceleration.

This nonlinear behavior was a significant concern during and after the test, beer-mse the frequency of this mode was known to be critical for the probes structural integrity, Prior loads analyses had determined that if the natural frequency of [his mode dropped more than 10% below pre-test predictions, the mode would couple more strongly with a 16 Hz axial mode of the Centaur upper stage, and loads in the probe would exceed levels used for design and for qualification testing, The nonlinearity made it impossible to extrapolate the test data [o flight levels, and even raised questions as to whether a linear loads analysis could be performed on the structure.

These issues were not resolved until January 1996, when a high level modal test was performed on the probe bounce mode. The details of this testing, and supporting analyses, are discussed in more detail in references [1 ,4].

7. SELECTION OF MODES FOR CORRELATION

After all of the test runs were completed, a total of 248 test modes had been identified by eight burst random tests, including high level runs. Many of these test modes were duplicate measurements of the same mode. A critical step at this point was the selection of the best modal parameters, including mode shapes, that should be retained for subsequent model correlation [5]. The criteria for this selection process included the following:

1. *Eliminate* duplicate *modes:* Distinct modes were identified by performing an orthogonality triple product $\Phi^T M \Phi$ using all 248 test modes, The mode shapes were first normalized so that the diagonal terms of this product were 1. In the resulting 248 by 248 matrix, off-diagonal terms near ± 1 indicate duplicate measurements of the same mode. Only one such mode was retained for model correlation.

2. *Select the highest level modes:* Where possible, mode shapes from the runs with the highest force levels were selected, so that the correlated model would best reflect the behavior of the structure at flight levels,

3. *Select the best quality modes:* In some cases, the mode shape from a high level run was clearly contaminated with noise, possibly due to nonlinear characteristics of the structure, This was evidenced by low modal confidence factors from the polyreference method, and by drastic differences in mode shape. In such cases, the advantage of using higher level data was outweighed by the questionable nature of the data, and a lower level shape was retained.

4. *Select a consistent set of modes:* In cases where there was no obvious discriminator between repeated measurements, selection was made so that a series of modes came from a single test run. By using a consistent source, potential problems of poor orthogonality between modes at different force levels were minimized.

These criteria were used to select 67 of the 248 modes in the frequency range 7.5 to 70 Hz. In several cases, test mode shapes were taken from burst random runs, hut frequencies were adjusted based on high level sine measurements.

8. TEST RESULTS

The first 30 test modes (selected from the full set of' modes as described in the previous section) are listed in Table 1. Representative mode shapes are shown in Figures 4 through 6. Effective mass of each test mode was computed, base.~ on the analytical mass matrix, and was used to select

'Table 1, First 30 test modes vs. analytical modes,

Test Mode	Freq (Hz)	Description	Pre-test TAM Mode No.	Pre-test TAM Freq (Hz)	Pre-test TAM Error (%)	Pre-test TAM Cross Ortho	Correlated TAM Mode No.	Correlated TAM Freq (Hz)	Correlated TAM Error (%)	Correlated TAM Cross Ortho	
1	7.511	Primary bending +X+Y	1	7.85	+4.5	99.3	1	7.44	-1.0	99.4	*
2	7,755	Primary bending +Y-X	2	8.18	+5.5	99%4	2	7,74	-0.1	99.4	*
3	15.522	Primary torsion	3	16.26	+4.7	92.8	3	15.55	+0,2	93.8	*
4	18.133	Probe bounce	4	18.95	+4.5	98.0	4	18.03	-0.6	98.0	*
5	20.47	RTG lateral	5	20.41	.0.3	90.3	5	20.37	-0.5	93.9	
6	20.95	Probe/RSP Y butterfly	8	21.28	+1.6	84.5	6	20.68	-1.3	91.2	+
7	21.34	RTG lateral, RSP bounce	6	20.49	-4.0	75.7	7	21.15	-0.9	93.4	+
8	21.82	RTG lateral, RSP bounce	11	21.97	+0.7	63.8	8	21.64	-0.8	97.0	
9	22.68	RTG lateral	7	20.60	-9.2	89.0	10	23.21	+2.3	97.2	
10	24.71	RTG vertical	10	21.85	-11.6	81.9	12	25.06	+1.4	77.3	
11	24.89	RTG vertical	9	21.41	-14.0	82.4	11	24.37	-2.1	80.5	
12	26.55	Second Y bending, RTG vertical	13	27.36	+3.0	78.1	13	26.59	+0.2	94.1	+
13	26.66	Probe experiment platform X	15	27.99	+5.0	72.3	15	27.48	+3.1	92.2	
14	27.47	Second torsion	15	27.99	+1.9	68.2	14	27.18	-1.0	86.2	
15	27.89	RTG vertical	12	22.58	-19.0	76.5	16	27.78	-0.4	94.7	
16	28.43	Hydrazine tank torsion	14	27.71	2.5	41.1	18	30.16	+6.1	83.3	
17	29.43	Second X bending	16	30.70	+4.3	82.0	17	29.62	+0.7	87.6	+
18	30.17	Helium, Hydrazine tanks bounce	63	62.50	+107.2	48.5	19	30.58	+1.4	87.3	+
19	31.55	Hydrazine tank bounce	21	35.92	+13.9	44.5	21	32.02	+1.5	86.1	+
20	32.11	FPP bounce	20	33.30	+3.7	65.9	22	32.47	+1.1	90.0	+
21	33.35	MEA +X+Y, HGA	21	35.92	+7.7	62.7	23	33.87	+1.5	67.1	
22	34.58	Probe front shield	18	32.72	-5.4	76.6	25	35.41	+2.4	84.8	
23	35.10	Ox tank -X, MEA +Y, HGA	23	36.67	+4.5	68.1	28	36.42	+3.8	73.2	
24	35.288	Ox tank -Y, MEA +X+Y, HGA	24	39.72	+12.6	41.2	27	35.92	+1.8	82.7	
25	36.30	Probe front shield torsion	19	32.84	-9.5	4949.6	2929	37.07	+2.1	51.4	
26	36.67	Fuel, Ox tanks -Z, Probe +torsion	22	36.30	-1.0	47.9	29	37.07	+1.1	89.1	+
27	37.28	Fuel, Ox tanks -Z, Probe front shld	21	35.92	-3.6	36.6	30	37.53	+0.7	88.9	*
28	38.27	RPWS	46	52.40	+36.9	54.1	52	51.89	+35.6	56.7	
29	39.33	Probe RY, RPWS	26	40.57	+3.1	54.8	33	40.50	+3.0	54.2	
30	39.34	Hydrazine tank lateral	29	42.42	+7.8	59.2	35	41.80	+6.2	37.8	

* Primary mode + Secondary mode

the most significant modes for later model correlation. Five test modes with effective mass at least 15% of the total rigid mass of the spacecraft were designated as primary modes (marked with an asterisk in Table I). Eight test modes with effective mass from 5% to 15% of the total rigid mass were designated as secondary modes (marked with a plus sign in Table 1).

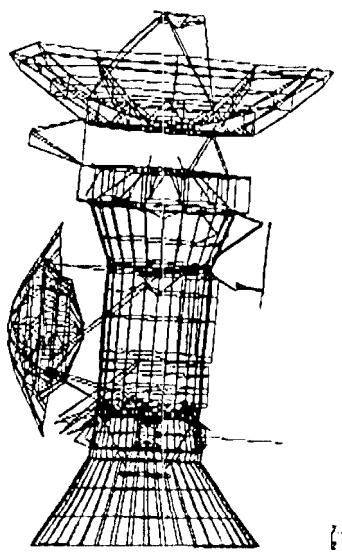

Figure 4. Test mode 1, 7.51 Hz, primary bending +X+Y.

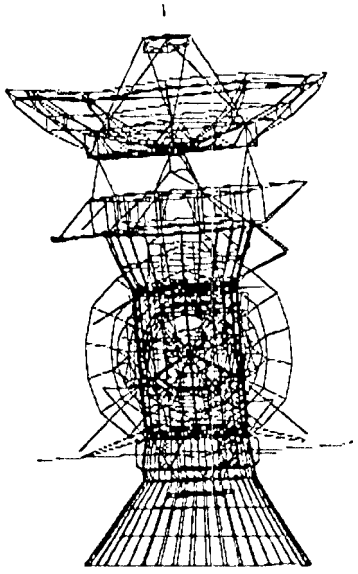

Figure 5. Test mode 2, 7.75 Hz, primary bending +Y-X.

Table 1 also compares the test modes with the pre-test TAM predictions, as well as the final TAM after model correlation was completed. After model correlation, the frequencies of all primary and secondary modes matched within 2%. Cross orthogonality goals (90% diagonal for primary modes. 85% diagonal for secondary modes) were satisfied with the exception of test mode 27. which was a primary mode and had cross orthogonality of 89%.

Self-orthogonality of the primary and secondary test modes is shown in Table 2, using the mass matrix of the correlated TAM. Most of the off-diagonal terms are small, but there were some terms related to test mode 1 8 that exceeded pre-test goals. This mode involves axial motion of two external tanks. The 32% orthogonality between test modes 18 and 19 is thought to be related to nonlinearities in the [sink supports.

Although not all orthogonality goals were completely satisfied, the test was considered very successful, considering the

Table 2. Orthogonality of primary/secondary test modes.

		Primary Modes					Secondary Modes							
		1	2	3	4	27	6	7	12	17	18	19	20	26
Mode	Freq	7.51	7.75	15.52	18.13	37.28	20.95	21.34	26.55	29.43	30.17	31.55	32.11	36.67
1	7.51		2	0	-3	0	-1	-2	1	-5	-4	-1	-2	-1
2	7.75	2		1	0	-1	3	0	-4	-2	2	-2	-1	-4
3	15.52	0	1		1	2	-3	1	-2	0	1	2	1	-2
4	18.13	-3	0	1		-1	3	0	0	0	-3	0	0	0
27	37.28	0	-1	2	-1		0	0	-1	0	-3	14	-3	9
6	20.95	-1	3	-3	3	0		-2	0	-1	-1	-1	-1	1
7	21.34	-2	0	1	0	0	-2		1	0	-2	0	0	1
12	26.55	1	-4	-2	0	-1	0	1		0	-13	3	3	1
17	29.43	-5	-2	0	0	0	-1	0	0		17	-9	0	-4
18	30.17	-4	2	1	-3	-3	-1	-2	-13	17		32	-9	2
19	31.55	-1	-2	2	0	14	-1	0	3	-9	32		0	14
20	32.11	-2	-1	1	0	-3	-1	0	3	0	-9	0		1
26	36.67	-1	-4	-2	0	9	1	1	1	-5	2	14	1	

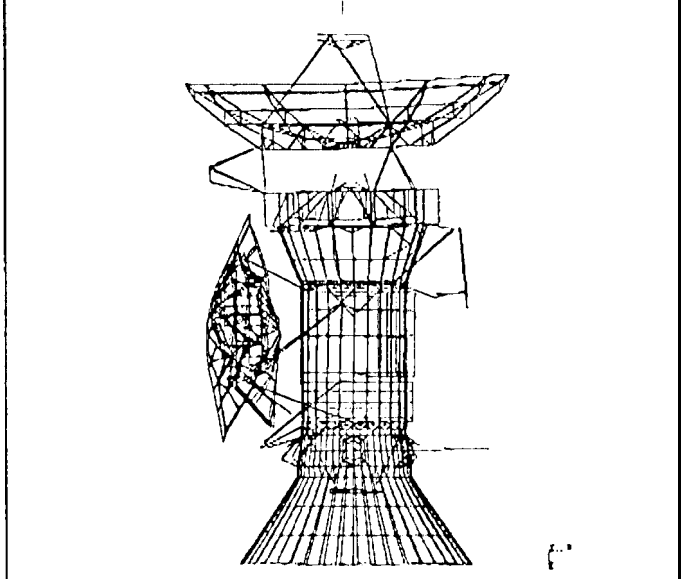

Figure 6. Test mode 4, 18.13 Hz., probe bounce,

dynamic complexity of the spacecraft. The primary axial mode (test mode 27) was particularly challenging, given the high mode number, and the participation of several appendages in the mode. The final model was approved for use in the final verification coupled load cycle,

9. LESSONS LEARNED

The Cassini modal test was a valuable experience for all in. vol *veal.* Some of the most important lessons for future large-scale modal test programs are outlined in the following paragraphs.

Do modal testing as early as practical. In the original project schedule, the Cassini modal test would have been performed on the flight spacecraft approximately 16 months before launch, with the test-verified model ready just 14 months before launch. Had this schedule been followed, there would have been no time to recover from the probe bounce mode nonlinearity, The decision by the Cassini project to put together a development test program (with modal testing over 2 years before launch) was very important, since it allowed time for thorough analysis, static testing, and high level modal testing to solve the problem. On launch vehicles other than the Titan IV, the overall timeline would be shorter, but the same principle should apply: leave enough time to deal with problems.

Use local coordinates sparingly. The idea of using local coordinates to optimize accelerometer usage seems like a good one, since it allows every measurement to be oriented in an optimum direction, In the real world, though, adding more local coordinate. systems means adding more chances for mistakes. In the Cassini test, 86 of the 135 node points were resolved in local coordinate systems, and a total of 34 different coordinate system definitions were used just for orientation of accelerometer axes. Several mistakes were made in entering the coordinate systems into the NASTRAN model. Also, the proliferation of local coordinates made it more, difficult to accurately identify orientations when installing accelerometers. Unless and until better tools arc available for minimizing these types of errors, it seems to be preferable to use local coordinate systems only where absolutely necessary, and instead to use adapter blocks and wedges to get accelerometers into the global coordinate system orientation.

Use an automated instrumentation management system. The Cassini modal test was another demonstration of the value of a barcode-based instrumentation management system. Other rhan the coordinate system problems described above, there were no errors due to mistyped serial numbers, sensitivities, or cable routing. JPL has used this system since 1992 for all large-scale testing programs.

Sine testing is still important. Not too long ago, virtually all modal tests were done using the tuned sine dwell technique. In recent years, the tremendous improvements in hardware and software have brought multipoint random testing [o the forefront. sometimes to the exclusion of sine testing. The Cassini test showed the value of' high level sine testing. Had we depended on the low and high level random test data, the frequency of the probe bounce mode would have been estimated at 20 Hz. Using high level sine testing, the final estimate was 18.1 Hz. This 10% drop in frequency re.subs in loads in the probe support that are approximately 50% higher than they would have been at 20 Hz.

10. CONCLUSIONS

The Cassini modal test was completed successfully, and the test results led to a test-verified dynamic model. Before [his happy conclusion. there were challenges from the structure (such as the probe bounce mode nonlinearity) and problems we brought on ourselves (such as our difficulties with coordinate systems). The experience gained from this test will help in planning future large-scale test programs.

ACKNOWLEDGEMENT

The work described herein was conducted by rhe Jet Propulsion Laboratory, California Institute of Technology, under contract with National Aeronautics and Space Administration.

REFERENCES

[1] Kenneth S, Smith and Chia-Yen Peng, "Cassini Spacecraft Modal Survey Report," *JPL Document D-13300*, January 22, 1996, Jet Propulsion Laboratory, California Institute of 'J'ethnology, Pasadena, CA.

[2] Kenneth S. Smith and Chin-Yen Peng, "Cassini Spacecraft Modal Survey Test Plan." *JPL Document D-12746*, June 12, 1995,

[3] Kenneth S. Smith and Chia-Yen Peng, "Air Mass Effects on The Cassini High Gain Antenna," *Proceedings of the 15th International Modal Analysis Conference*, Or lando, Florida, February 3-6.1997.

[4] Kelly Carney, Isam Yunis, Kenneth S. Smith, and Chia-Yen Peng, "Nonlinear Dynamic Behavior in the Cassini Spacecraft Modal Survey," *Proceedings of the 15th International Modal Analysis Conference,* Orlando, Florida, February 3-6, 1997.

[5] Kenneth S. Smith and Michelle Coleman, "Cassini Spacecraft Model Correlation Report," *JPL Document D-13610*, June 15, 1996.